Model Predictive Direct Power Control Based on Improved T - type Grid Connected Inverter

Guoliang Yang , *Member, IEEE*, Shuai Hao, Chuntian Fu,and Zhe Chen

***Abstract*—In this paper, the improved T-type three-level topology can significantly reduce the conduction loss in zero states compared with the traditional T-type three-level topology. In the DQ rotating coordinate system, a control method combining the model predictive algorithm and the direct power control is proposed. This control method divides 27 kinds of switch states into two groupsand decides which group of switch states is to be scrolled optimally by comparing the two capacitor voltages on the DC side. This method reduces the computational burden by reducing the number of rolling optimization under the condition of ensuring the neutral point voltage balance. Compared with the traditional multilevel model predictive control, the method eliminates the need of predicting the neutral point voltage as well as the cost function computation, and the control method is more direct and effective. Simulation and experimental results show that the proposed model predictive direct power control (MPDPC) method based on the improved T-topology can improve system robustness, fast dynamic response, wide operating range and stability.**

***Index Terms*—Improved T-type inverter,Model predictive direct power control, neutral point voltage balance, three-level,Grid- connected.**

I. INTRODUCTION

THE inverter is a key part of the grid-connected system. It has high requirements on the quality and conversion efficiency of the waveform. A control method with good performance is very important. Improved T-type three-level inverter not only inherits the advantages of the traditional T-type three-level converter such as less component count,no clamping diodes through the current path,but also has more excellent performance in conduction loss. Compared with the traditional T-type three-level inverter topology, the improved T-type inverter reduces conduction losses by 90% under zero-vector conditions, which is equivalent to a total loss reduction of 30% [1].

MPC (Model Predictive Control) has the advantages of fast dynamic response, strong anti-interference ability, the low requirement on the model and the obvious advantages in dealing with nonlinear systems and multi-control targets. Ever since its inception, it has been constantly welcomed by industries system with strong disturbances and time-varying large inertia. It has been widely used in power electronics [2], motor-driven [3], solar wind power conversion [4],[5] and another control system. However, the traditional model predictive control increases dramatically as the number of levels increases and the number of control objectives increases. Direct power control has the advantages of good robustness, fast dynamic response, and a simple control structure. It has been widely used in practice. In this paper, the combination of model predictive control and direct power control not only inherits the advantages of good robustness of direct power control and simple control structure but also achieves the control of neutral point balance and constant power output.

Literature [6] proposed a finite-state model predictive direct power control method for photovoltaic grid-connected inverters. The system outputs the active and reactive power to predict, according to the cost function, choose to minimize the output power ripple voltage vector and the role of the next sampling period. Literature [7] established the power predictive model of PV grid-connected inverter in rotating DQ coordinate system. The sum of the absolute value of the predicted power and the given power error is selected as the value function and the optimal space voltage vector is selected according to the power prediction model to realize the control of the inverter. According to [8], a three-level inverter is used to determine the sector where the synthesized vector is located according to the power mathematical model of the grid-connected inverter and the finite basic space voltage vector of the three-level inverter. Based on the model predictive control target Function of the optimal principle, calculate the three basic voltage vector within the sector of the action time to determine the order of action, modulation so that the instantaneous active, reactive power minimum error trigger pulse. In [9], the terminal sliding mode variable structure is applied to the direct power control (DPC) of doubly fed induction generator (DFIG) system. The sliding mode variable structure and space voltage vector pulse width modulation (SVPWM) Control two-phase rotor voltage direct control of the system stator side of the active and reactive power, omit the current control, thus simplifying the control

Manuscript receieved February 6, 2018; revised July 9, 2018; accepted August 28, 2018; Date of current version September15, 2018. This work was supported by the National Natural Science Foundation of China under Grant No.61873226 , the Science And Technology project of Hebei province, China, under Grant No.15214318, and the University research program of Xinjiang Uygur Autonomous Region, China ,under Grant No.XJEDU2016S114.

GuoliangYang, ShuaiHao, Chuntian Fu are with the Department of Electrical Engineering and Automation, Yanshan University, Qinhuangdao, 066004, China (e-mail: y99ygl@ysu.edu.cn).

ZheChen is with the Department of Energy Technology, Aalborg University,Aalborg 9220, Denmark(e-mail: zch@et.aau.dk).

structure. Literature [10] proposed a model predictive direct power control (MPDPC) that regulates the instantaneous real power delivered to the grid within a set of symmetric boundaries while minimizing the switching frequency of the converter. Use the multi-step prediction time domain to distinguish MPDPC from FCS-MPC based policies. Literature [11] proposed the AC / DC converter that uses the model to predict the direct power control (MPDPC), the dynamic performance is improved. Dynamic performance of system dynamics caused by mutual interference is improved by reconfiguring cost functions with weighting factors. Literature [12] proposed a direct vector control (LC-MPDPC) strategy based on a three-vector low-complexity DFIG model for wind energy applications, which significantly improves the steady-state performance and achieves freedom control. Literature [13] proposed a deadbeat direct power control strategy when the grid voltage is unbalanced. This strategy omits the current inner loop, so it does not need complicated reference current calculation and avoids using multiple PI regulators and multiple PI parameters Difficult to set the difficulty of achieving active and reactive direct control, fast response.

In the study of the three-level inverter, the inherent flaw of its topology makes the neutral point voltage balance has been a hot research, none of the above-mentioned references to the neutral point voltage control. Literature [14] proposed to use the hysteresis comparison method and the balance factor method to balance the neutral point voltage control, hysteresis comparison method and balance factor method to balance the neutral point voltage in low-modulation system, and balance factor method to balance high-modulation system The neutral point voltage; literature [15] studied a model based on the predictive control of the neutral point potential balance control method, the current sample values to calculate the predicted value, while taking DC bus neutral point current, the neutral point potential deviation; Optimize the performance index function composed of the square error between the prediction current and the reference current and the deviation value of the neutral point potential, and select the switch state with the smallest function index function to act on the inverter in the next sampling period to achieve the neutral point potential balance control. Literature [16] proposed using a fuzzy control algorithm to control the neutral point voltage, designed a fuzzy controller, and analyzed the principle of distribution of balance factor. In [17], by introducing the change of voltage vector itself during the neutral point voltage offset and the redundant vector action time caused by the balancing algorithm, the error curve of the SMC is obtained. Then the small balance factor of neutral point voltage is introduced into the selection of vector and the calculation of action time, and the small balance factor is used to adjust the vector action time.

In this paper, a model predictive direct power control based on the improved T-type three-level inverter is proposed. In the DQ rotating coordinate system, the decoupling of active power and reactive power is realized, and 27 voltage vectors are divided into two groups according to the mid-voltage state. This method not only achieves neutral point voltage balance but also reduces the number of rolling optimization and avoids the prediction of neutral point voltage, which greatly reduces the computational cost and achieves rapidity.

II. IMPROVED T-TYPE THREE-LEVEL INVERTER

This article adopts an improved T-type three-level converter structure, shown in Figure 1. The topology uses two inverting series Cool MOSFET instead of the traditional T-type three-level IGBT + diode bidirectional switch, which are in series by back to back. The improved structure greatly reduces the conduction loss. Replacing the IGBT + diode with two reverse series-connected Cool Mosfets in a bidirectional switch, a parallel branch is constituted of the four switches, which to reduce the equivalent resistance. With current flowing through two reverse-parallel Cool Mosfets. it is the absence of a diode in this current path. The zero-vector conduction loss is reduced by 90% and the total transmission loss is reduced by about 30% [1]. In this way, in the low voltage wind power system, the transmission loss of the switch device is greatly reduced. The new Mosfet's "hyperlink" structure is adopted in the Cool Mosfet. Compared with the traditional low on-resistance Mosfet, it has the advantages of excellent characteristics of switching, high frequency and the like.

In the control strategy of each switch, although the number of the power switches in per phase increases from four of the conventional T-type topologies to six, the signals from the switches of Sx1-1 and Sx1-2, Sx2-1 and Sx2-2 are the same respectively, so the switch state of each phase is still four kinds.

The current runs through two reverse connected N-channel high-voltage power MOSFET in O state (0110). Therefore, no parasitic diode is required in the loop, even in non-unity power factors (ie, the current is still present in the voltage shutdown). As can be seen from Fig. 2, in the non-zero state region, the conduction losses between the improved T-type topology and the conventional T-type three-level inverter are the same, which are conducted through the switches Sx1 and Sx4, respectively. But in the O state, the current passes through two parallel channels consist of four N-channel enhancement high-voltage power MOSFETs, which are two forward connections and the other two reverse connections. As a result, the equivalent on-resistance is reduced by half. Therefore, no freewheeling diode is required in the O-state current loop.

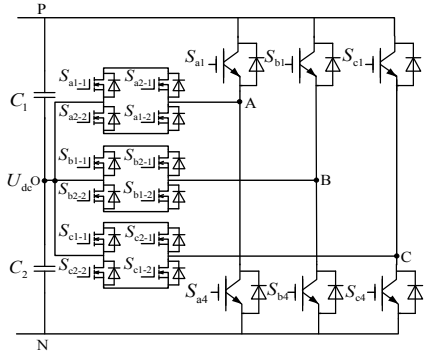

Fig.1 Improved T-type three- level inverter topology

This article has been accepted for publication in a future issue of this journal, but has not been fully edited. Content may change prior to final publication. Citation information: DOI 10.1109/JESTPE.2018.2871113, IEEE Journal of Emerging and Selected Topics in Power Electronics

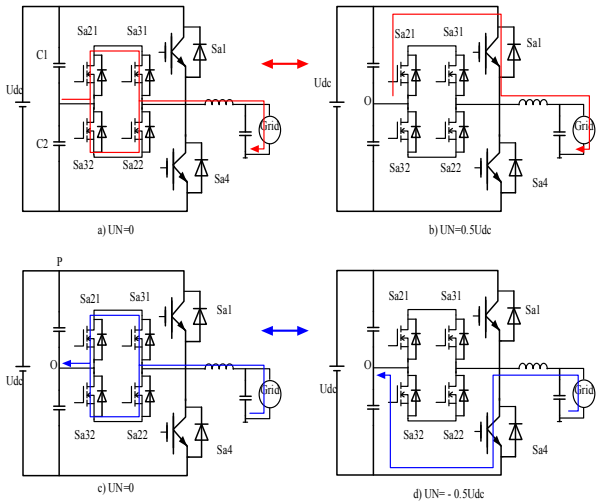

Fig.2 Improved T-inverter four working conditions

$$P_{\mathrm{S1,S2-cond}}=\frac{1}{T}\int_{0}^{\phi}v_{\mathrm{FW}}\cdot\left[\frac{P_{\mathrm{out}}\cdot\sqrt{2}\cdot\sin(\omega t)}{U_{\mathrm{g}}}\right]\cdot m\cdot\sin(\omega t)dt+\frac{1}{T}\int_{\phi}^{\pi}v_{\mathrm{ce}}\cdot\left[\frac{P_{\mathrm{out}}\cdot\sqrt{2}\cdot\sin(\omega t)}{U_{\mathrm{g}}}\right]\cdot m\cdot\sin(\omega t)dt \tag{1}$$

$$P_{\mathrm{S1c-1,S1c-2,S2c-1,S2c-2-cond}}=\frac{1}{T}\left[\int_{0}^{T}r_{\mathrm{on}}\cdot\frac{1}{2}\cdot\frac{P_{\mathrm{out}}\cdot\sqrt{2}\cdot\sin(\omega t)}{U_{\mathrm{g}}}\right]^{2}\times\left[1-m\cdot\sin(\omega t)\right]dt \tag{2}$$

Where ϕ, v_{FW}, U_{g}, P_{out}, T, r_{on} and v_{ce} respectively, represent phase angle, IGBT body diode forward voltage, grid voltage, output power, power grid cycle, Cool MOSFET on resistance and IGBT drive voltage. From [1] we can see, Cool MOSFET conduction losses at different power factor are constant.

III. GRID SYSTEM MATHEMATICAL MODEL

Decoupling of active power and reactive power can be achieved in theDQ rotating coordinate system [20]. The ω is taken as the rotating angular velocity of the DQ rotating coordinate system, and the dynamic equation of the DQ rotating coordinate system of the three-phase inverter is obtained

$$\begin{cases}L\dfrac{di_d}{dt}=u_d-e_d-Ri_d-\omega i_q\\ L\dfrac{di_q}{dt}=u_q-e_q-Ri_q+\omega i_d\end{cases} \tag{3}$$

Where, i_{d}, i_q is the output current component of the three-phase inverter in theDQrotating coordinate system; u_d, u_q is the output voltage component of the three-phase inverter in the DQ rotating coordinate system; e_d, e_q is the grid voltage component in DQ rotating coordinate system.

Discrete formula (3) to get the discrete dynamic equation:

$$\begin{cases}i_d(k+1)=\left(1-\dfrac{T_sR}{L}\right)i_d(k)+\dfrac{T_s}{L}\left[u_d(k+1)-e_d(k)\right]-\omega T_s i_q(k)\\ i_q(k+1)=\left(1-\dfrac{T_sR}{L}\right)i_q(k)+\dfrac{T_s}{L}\left[u_q(k+1)-e_q(k)\right]+\omega T_s i_d(k)\end{cases} \tag{4}$$

Where, T_s is the sampling time.

The instantaneous active power P and reactive power Q in DQ rotating coordinate system of the three-phase inverter can be expressed as

$$\begin{cases}P(k+1)=e_d(k+1)i_d(k+1)+e_q(k+1)i_q(k+1)\\ Q(k+1)=e_q(k+1)i_d(k+1)-e_d(k+1)i_q(k+1)\end{cases} \tag{5}$$

As the sampling frequency is much higher than the grid frequency, in generally a few thousand to tens of thousands of hertz, it can be considered that the grid voltage is constant in a sampling period, that is

$$\begin{cases}e_d(\mathrm{k}+1)=e_d(\mathrm{k})\\ e_q(\mathrm{k}+1)=e_q(\mathrm{k})\end{cases} \tag{6}$$

Available from (4), (5) and (6)

$$\begin{cases}P(k+1)=\left[\left(1-\dfrac{T_sR}{L}\right)i_d(k)+\dfrac{T_s}{L}\left(u_d(k+1)-e_d(k)\right)-\omega T_s i_q(k)\right]e_d(k)\\ \qquad+\left[\left(1-\dfrac{T_sR}{L}\right)i_q(k)+\dfrac{T_s}{L}\left(u_q(k+1)-e_q(k)\right)+\omega T_s i_d(k)\right]e_q(k)\\ Q(k+1)=\left[\left(1-\dfrac{T_sR}{L}\right)i_d(k)+\dfrac{T_s}{L}\left(u_d(k+1)-e_d(k)\right)-\omega T_s i_q(k)\right]e_q(k)\\ \qquad-\left[\left(1-\dfrac{T_sR}{L}\right)i_q(k)+\dfrac{T_s}{L}\left(u_q(k+1)-e_q(k)\right)+\omega T_s i_d(k)\right]e_d(k)\end{cases} \tag{7}$$

In phase-locked technology, the grid voltage e_d is set on the d-axis in the DQ rotating coordinate system, so the active power P and the reactive power Q are reduced to

$$\begin{cases}P(k+1)=e_d(k+1)i_d(k+1)\\ Q(k+1)=-e_d(k+1)i_q(k+1)\end{cases} \tag{8}$$

Available from (7) and (8)

$$\begin{cases}P(k+1)=\left(1-\dfrac{T_sR}{L}\right)P(k)+\dfrac{T_s}{L}\left[u_d(k+1)e_d(k)-e_d^2(k)\right]\\ \qquad-\omega T_s e_d(k)i_q(k)\\ Q(k+1)=\left(1-\dfrac{T_sR}{L}\right)Q(k)-\dfrac{T_s}{L}u_d(k+1)e_d(k)\\ \qquad-\omega T_s e_d(k)i_d(k)\end{cases} \tag{9}$$

Equation (9) is the output of active power and reactive power when the system is rolling optimized

This article has been accepted for publication in a future issue of this journal, but has not been fully edited. Content may change prior to final publication. Citation information: DOI 10.1109/JESTPE.2018.2871113, IEEE Journal of Emerging and Selected Topics in Power Electronics

IV. MODEL PREDICTIVE DIRECT POWER CONTROL STRATEGY

A. Improved T-Type Voltage Balance Control

The current control of the voltage balance is divided into two main categories. One kind is in the modulation in the control, such as literature [18] by sampling the neutral point voltage, and the limit range of modulation wave bias adjustment coefficient is online calculated according to the modulation ratio, the output current amplitude, output power factor angle. Next, the optimal adjustment coefficient is searched to achieve the dynamic adjustment of the modulation wave offset so as to achieve the neutral point voltage balance control on different load conditions. The other is to control the neutral point voltage balance by setting the corresponding weighting factors in the objective function on the model predictive control [14].

The model predictive control calculates the power of each space voltage vector in the rolling optimization process. Its goal is to find a space voltage vector that brings its power output value closest to the power reference. If at this time one of the small vectors meets the requirement, such as V_2, which corresponding to the two switch states (1 1 0,0 0 -1) are in line with the requirements. If the state of the switch 110 in the rolling optimization is before 0 0 -1, the system will always select 1 1 0 as the optimal switching state and the switch state 0 0 -1 will never be selected according to the optimal principle On the side of the capacitor has been in a state of discharge, a long time there will be neutral point voltage imbalance situation. So according to the inherent characteristics of the model predictive control, the neutral point voltage must be controlled to maintain its balance.

The improved T-type three-level inverter has 27 space voltage vectors, as shown in Figure 3. Among them, the small vector and the zero vector all contain redundant vectors, which lays the foundation for the study of neutral point balance. In a small vector, 12 kinds of switch states generate 6 kinds of space voltage vectors, that is, each kind of space voltage vector corresponds to 2 kinds of switch states. One of the switch states discharges the upper capacitor and the other discharges the lower capacitor. As shown in Figures 4 (a) and 4 (b), the small vectors 100, 110, 010, 011, 001 and 101 reduce the voltage of the upper capacitor. The small vectors 0-1-1,00-1, -1-10, -100 , -10-1,0-10 will reduce the voltage of the lower capacitor.

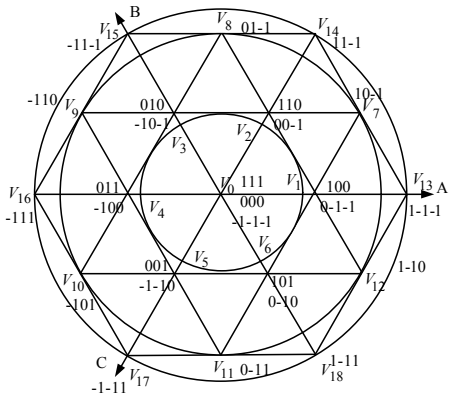

Fig.3 The improved T-type three-level inverter space voltage vector

For the zero vector and the large vector, the neutral point potential is not affected because the zero vector and the large vector do not control, as shown in Figure 4 (c) and Figure 4 (d) below. In figure 4 (e), the vector will also affect the neutral point potential, but the impact on the neutral point potential is uncertain, so it is difficult to control the neutral point of the balance.

According to the above rules, In this paper, 27 space voltage vectors are divided into two groups of 21 space voltage vectors, as shown in Figure 5. According to the state of the neutral point voltage, the corresponding space voltage vector group is selected to be scrolled optimally, thus reducing the rolling optimization coefficient to a certain extent and improving the system response speed.

In addition, because of this rule, the system will no longer have to predict the neutral point voltage trend, which also reduces the amount of calculation and improve the response speed of the system.

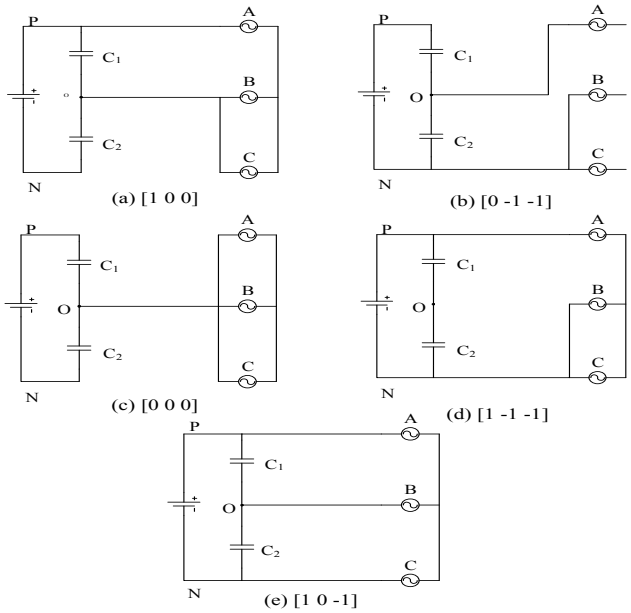

Fig.4 Effect of the improved T-type three-level inverter vector on voltage neutral point balance

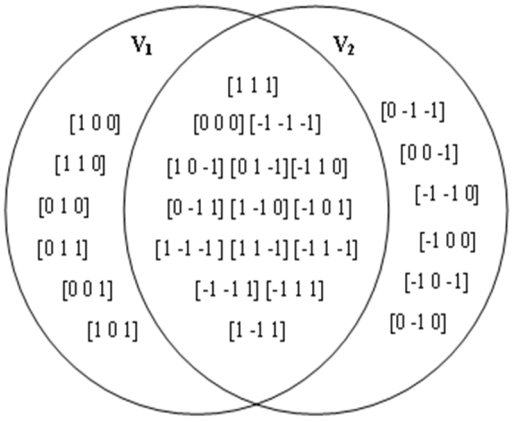

Fig.5 Space voltage vector grouping map

This article has been accepted for publication in a future issue of this journal, but has not been fully edited. Content may change prior to final publication. Citation information: DOI 10.1109/JESTPE.2018.2871113, IEEE Journal of Emerging and Selected Topics in Power Electronics

B. System Control Program

The model predictive direct power control scheme as shown in Figure 6. External given active power P^* and reactive power Q^*, in order to achieve unity power factor inversion, the reactive power reference Q^* is usually set to zero. According to the instantaneous power theory, the active power $P(k)$ and the reactive power $Q(k)$ can be obtained at the time k; $e(k)$ is the electromotive force of the grid; $u_i(k)$ is the output voltage of the inverter and can be obtained by the predictive model. All the predictive values $P(k+1)$, $Q(k+1)$ at the moment $k+1$, corresponding to the voltage vector $u_i(k)$. The cost function is used to compare the power setpoint with each predicted value. It chooses the voltage vector $u_i(k)$ that minimizes the cost function and applies its corresponding switch state.

In this paper, the output side of the active power, reactive power, and voltage dividing capacitor neutral point potential as the control target, the objective function of the improved T-type inverter can be obtained:

$$g = \left|P_{ref} - P(k+1)\right| + \left|Q_{ref} - Q(k+1)\right| \tag{10}$$

Figure 7 is a flowchart of the model predictive direct power control scheme of the improved T-type three-level inverter. The system collects the three-phase currents i_a, i_b, i_c and the three-phase voltages e_a, e_b, e_c of the power grid from the output side of the improved T-type inverter. The output current DQ coordinate system i_d, i_q and grid voltage, e_d, e_q are obtained by coordinate transformation. Then the active power $P(k)$ and the reactive power $Q(k)$ at the current time are calculated, and the corresponding space voltage vector group is selected and scrolled optimally by judging the state of the current neutral point voltage. The space voltage vector group V_1 is selected when the voltage across the upper capacitor is greater than the voltage across the lower capacitor, and the space voltage vector group V_2 is selected when the voltage across the upper capacitor is less than the voltage across the lower capacitor. The specific voltage vector and switch status are shown in Table I.

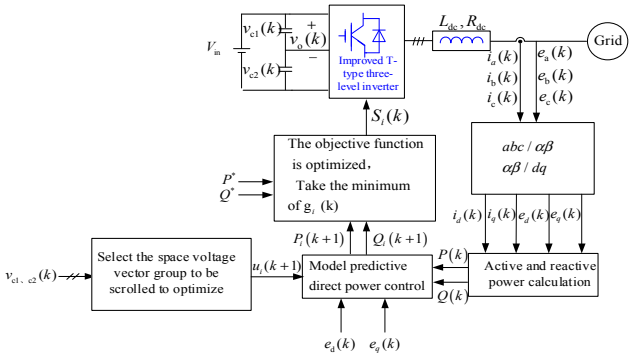

Fig.6 Model predictive direct power control scheme

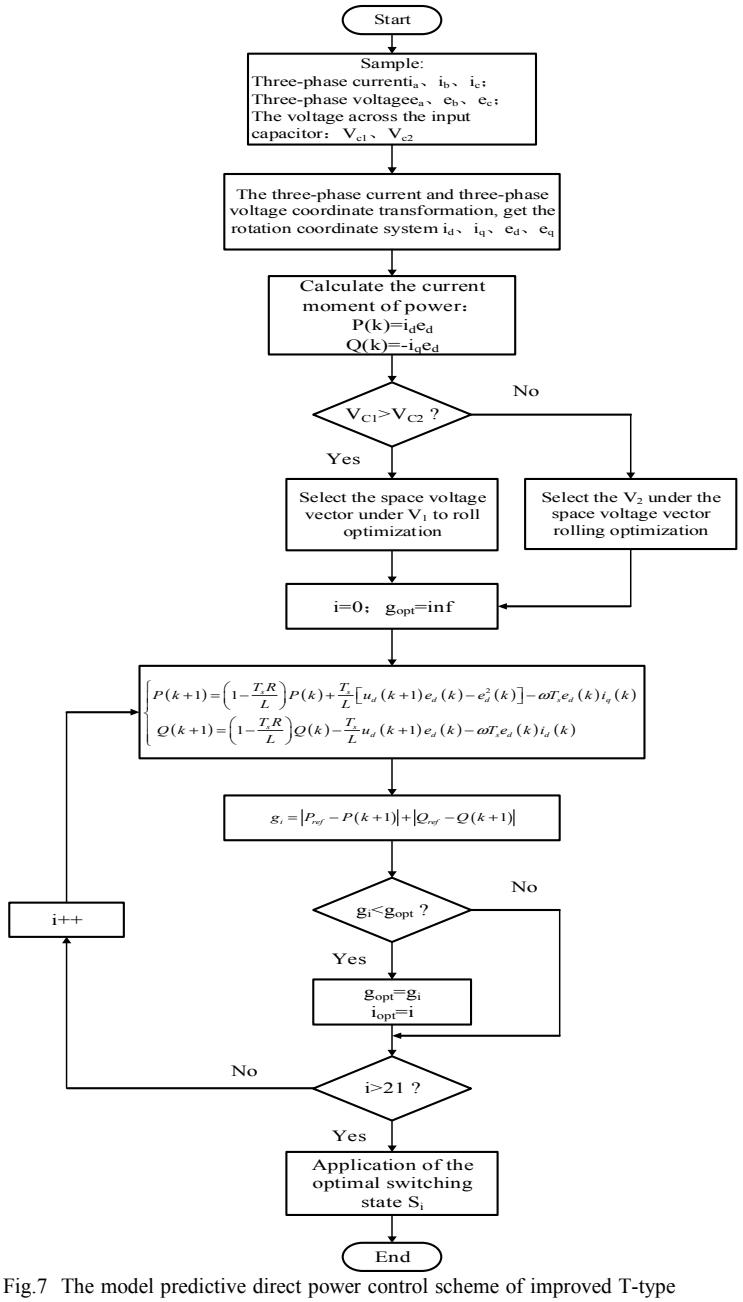

Fig.7 The model predictive direct power control scheme of improved T-type three-level inverter

The corresponding $P(k+1)$ and $Q(k+1)$ are generated by the different $U_d(k+1)$ in the predictive model (7) due to different switching states.

TABLE I
SSPACE VOLTAGE GROUPING SWITCH

Space voltage vector set	V_1	V_2
Zero vector	[1 1 1] [0 0 0] [-1 -1 -1]	
Small vector	[1 0 0] [1 1 0] [0 1 0] [0 1 1] [0 0 1] [1 0 1]	[0 -1 -1] [0 0 -1] [-1 -1 0] [-1 0 0] [-1 0 -1] [0 -1 0]
Medium vector	[1 0 -1] [0 1 -1] [-1 1 0] [0 -1 1] [1 -1 0] [-1 0 1]	
Big vector	[1 -1 -1] [1 1 -1] [-1 1 -1] [-1 -1 1] [-1 1 1] [1 -1 1]	

This article has been accepted for publication in a future issue of this journal, but has not been fully edited. Content may change prior to final publication. Citation information: DOI 10.1109/JESTPE.2018.2871113, IEEE Journal of Emerging and Selected Topics in Power Electronics

According to the cost function (9) find the optimal switching state closest to the given active power, to improve the T-type inverter.

V. SIMULATION AND EXPERIMENT

A. Simulation

In order to verify that the control performance of the modelpredictive direct power control method in the improved T-type inverter, the control model of the three-phase grid-connected inverter is built in the MATLAB / Simulink simulation environment, and the rapidity and stability of the control method are verified By changing the power reference.In the simulation model, the grid voltage is three phase symmetrical and works in the unit-factor power mode. Frequency is 50Hz, simulation parameters are set as shown in Table II.

Figure 8 shows the output current of the improved T-type three-level inverter. At the moment t = 0.1s, the output active power is jumping from 8kW to 10kW. It can be seen from the figure 9 that the system can quickly reach steady state, It can be seen that the settling time is within 0.75ms.

Figure 10 shows the three-phase output voltage of the inverter. Since the output of the inverter is connected to the power grid, the amplitude and phase of the output are clamped by the power grid with a phase difference of 120 ° and an amplitude of 311V.

TABLE II
MODEL PREDICTIVE CONTROLLER SIMULATION PARAMETER SETTING

Parameter	Value
DC input voltage V_{in} (V)	200
Grid phase voltage amplitude e_{peak} (V)	311
Grid voltage frequency f (Hz)	50
Sampling frequency f_s (kHz)	50
Active power P (kW)	10
Reactive power Q (kvar)	0
Inverter side inductance L (mH)	8
DC side capacitor $C_{1,2}$ (mF)	4
Filtering capacitance C (μF)	10
Capacitor Series Resistance R_d (Ω)	1.5

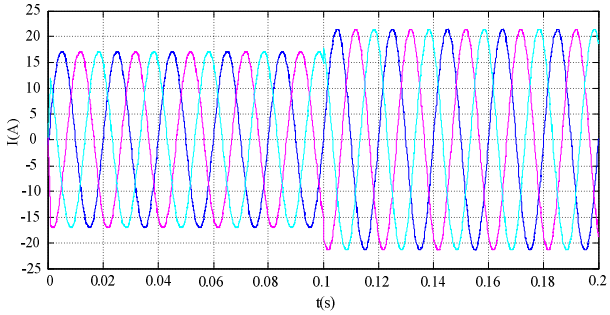

Fig.8 Three-phase current waveform

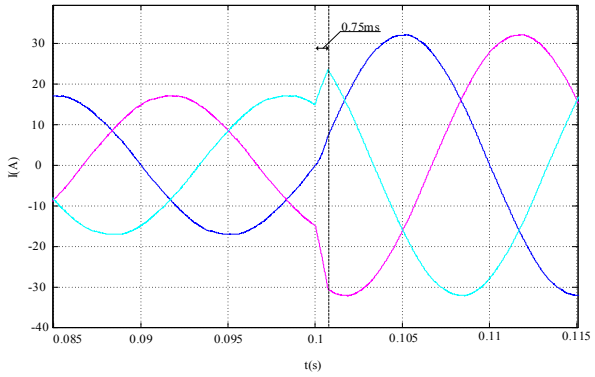

Fig.9 The amplification waveform of Figure 7 at 0.1s

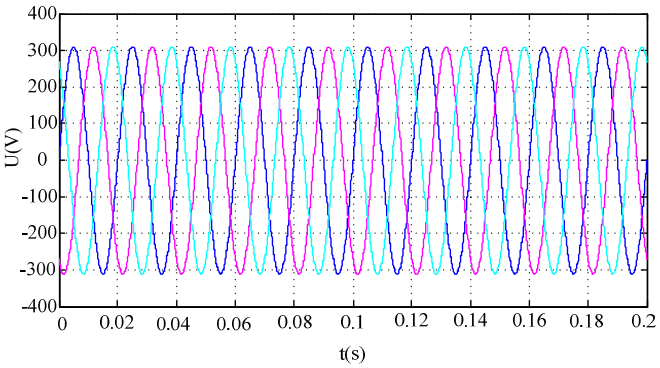

Fig.10 the three-phase output voltage of the inverter

Figure 11 shows the neutral point voltage balance waveform. As can be seen from the figure, the neutral point voltage is 399.5V. even when the reference value is in fluctuation at t = 0.1s, this voltage is 399.4V, which is still stable at around 400V. The accuracy is up to 99% and the voltage ripple coefficient of 0.05%, which lay a solid foundation for system stability and high-precision operation.

Figure 12 shows the dynamic waveform of active and reactive power injected into the grid. At the moment t = 0.1s, the active reference power increases from 8kW to 10kW, and the system can respond quickly and accurately, which fully demonstrates the effectiveness and accuracy of the model predictive direct power control.

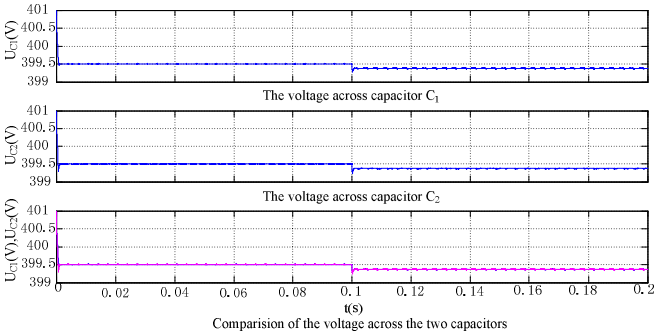

Fig.11 Neutral point voltage balance waveform

This article has been accepted for publication in a future issue of this journal, but has not been fully edited. Content may change prior to final publication. Citation information: DOI 10.1109/JESTPE.2018.2871113, IEEE Journal of Emerging and Selected Topics in Power Electronics

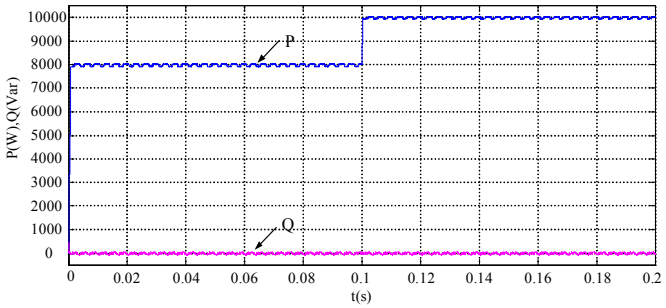

Fig.12 The active and reactive power waveform

The following TableIII shows the specific switching loss data obtained by simulating from the traditional T-type three-level inverter and the improved T-type three-level inverter under different power conditions with the same control method.

TABLE III
COMPARISON OF SWITCHING LOSS BETWEEN IMPROVED T-TYPE INVERTER AND TRADITIONAL T-TYPE INVERTER UNDER DIFFERENT LOADING CONDITIONS

Power Conditions (Active power)	Switching loss rate (Improved-type)	Switching loss rate (Traditional T-type)
5 kW	1.1%	1.3%
6 kW	1.2%	1.45%
7 kW	1.3%	1.6%
8 kW	1.35%	1.75%
9 kW	1.45%	1.88%
10 kW	1.5%	1.95%
11 kW	1.55%	2.14%
12 kW	1.66%	2.28%
13 kW	1.7%	2.5%
14 kW	1.8%	2.54%
15 kW	1.85%	2.6%

The switching loss of the MOS switch tube is calculated with a reference to Infineon's cool mosfet whose model is SPW47N65C3 (650V/47A) with a pass resistance of 70m .Since the on-state loss of the IGBT is related to temperature, Ic current, gate voltage and other factors, the on-state resistance cannot be determined, or the IGBT has no on-state resistance. The on-state loss is expressed by the on-state voltage drop, which is generally 2-4V. Therefore, when simulating, we give a reasonable resistance so that the voltage drop is between 2-4V.The simulation environment is reasonable, so the loss analysis data obtained is valid.

The calculation efficiency formula is shown in formula (11)

$$E = \frac{P_{out}}{P_{in}} = \frac{3U_a \times I_a}{U_{dc} \times I_{dc}} \times 100\% \quad (11)$$

Where Pout is the output active power of the inverter, Pin is the input active power of the inverter, Ua is the phase voltage of phase A, Ia is the phase current of phase A, Udc is the voltage on the DC side,Idc is the voltage on the DC side.

The calculated specific data is shown in Table IV.

Figure 13 is a chart of efficiency comparison between the improved T-type three-level inverter and T-type three-level inverter. It can be seen from the figure that in the range of active power from 5kW to 15kW, the working efficiency of the improved T-type inverter is better than that of the T-type inverter at all power levels, which proves that the low loss characteristics of the improved T-type three-level inverter.

TABLE IV
COMPARISON OF EFFICIENCY BETWEEN IMPROVED T-TYPE INVERTER AND TRADITIONAL T-TYPE INVERTER UNDER DIFFERENT LOADING CONDITIONS

Power Conditions (Active power)	Efficiency (Improved-type)	Efficiency (Traditional T-type)
5 kW	98.90%	98.70%
6 kW	98.80%	98.55%
7 kW	98.70%	98.40%
8 kW	98.65%	98.25%
9 kW	98.55%	98.12%
10 kW	98.50%	98.05%
11 kW	98.45%	97.86%
12 kW	98.34%	97.72%
13 kW	98.30%	97.50%
14 kW	98.20%	97.46%
15 kW	98.15%	97.40%

Figure 13 is a chart of efficiency comparison between the improved T-type three-level inverter and T-type three-level inverter. It can be seen from the figure that in the range of active power from 5kW to 15kW, the working efficiency of the improved T-type inverter is better than that of the T-type inverter at all power levels, which proves that the low loss characteristics of the improved T-type three-level inverter.

B. Experiment

In order to verify the feasibility of the proposed control method, an experimental platform as shown in Figure 14 was set up. The specific experimental parameters are shown in TableV.

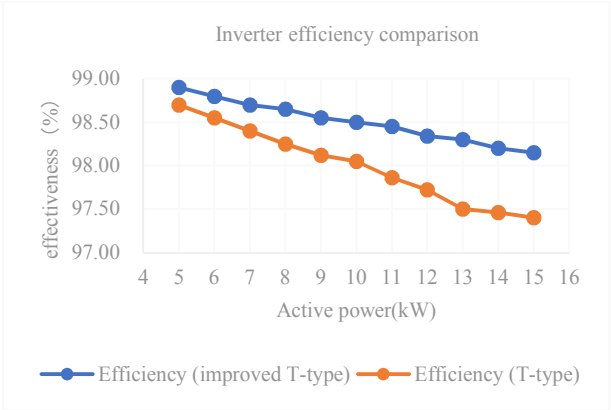

Fig.13 Efficiency comparison between improved T-type three-level inverter and T-type three-level inverter

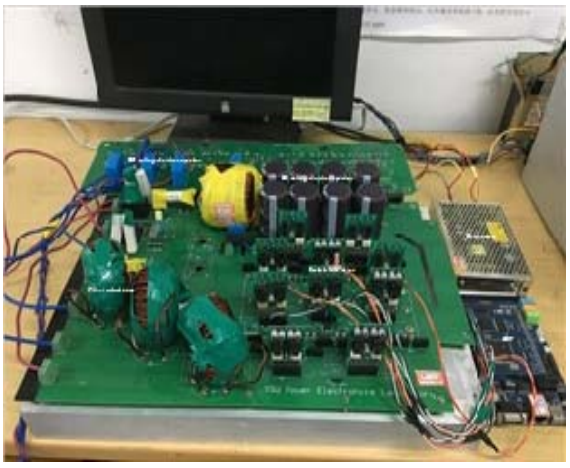

Fig.14 Improved T-type three-level inverter experimental platform

This article has been accepted for publication in a future issue of this journal, but has not been fully edited. Content may change prior to final publication. Citation information: DOI 10.1109/JESTPE.2018.2871113, IEEE Journal of Emerging and Selected Topics in Power Electronics

TABLE V
MODEL PREDICTIVE DIRECT POWER CONTROL CONTROLLER EXPERIMENTAL PARAMETER SETTINGS

Parameter	Value
DC input voltage V_{in} (V)	200
Active power P (kW)	10
Reactive power Q (kvar)	0
Inverter side inductance L (mH)	1.56
DC side capacitor $C_{1,2}$ (mF)	4
Filtering capacitance C (μF)	20
Capacitor Series Resistance R_d (Ω)	1.5
CoolMOS	SPW47N65C3 (650V/47A)
IGBT	IRG4PH40UD2-E (1200V/41A)

Figure 15 shows the DC voltage waveform and the inverter-side filter voltage waveform. As can be seen from the figure, the DC bus voltage input 200V, the unilateral bus voltage up to 100V, the inverter output voltage at this time to 80V. In order to ensure the safety of experimental operation, the AC voltage regulator voltage amplitude is also transferred to 80V, then synchronization control and grid connect.

Figure 16 shows the voltages on capacitors C1 and C2. It can be seen that the voltages on the two capacitors are equal and the neutral point potentials are balanced. This experiment mainly verifies the feasibility of the model predictive control scheme for neutral- point voltage balance based on improved T-type three level inverter.

Figure 17 shows the output filtered AB line voltage experimental waveform and unfiltered AB line voltage experimental waveform. It can be seen from the figure, the line voltage between A phase and B phase is five levels before filtering, the output waveform shows smooth after filtering.

Figure 18 shows the filtered waveform of the three-phase output voltage and a single-phase output current from the inverter. This experiment mainly verifies the feasibility of the control method. The reactive power loss caused by filter and line impedance is borne by the power grid, and there is a small phase angle difference. This verifies the feasibility of the model predictive direct power control scheme.

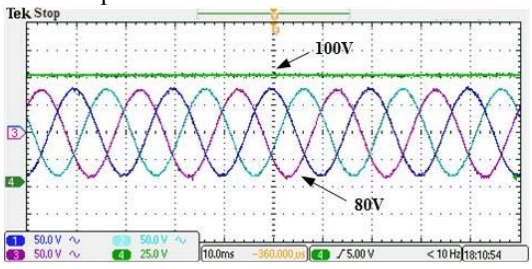

Fig.15 DC voltage waveform and inverter side filter voltage waveform

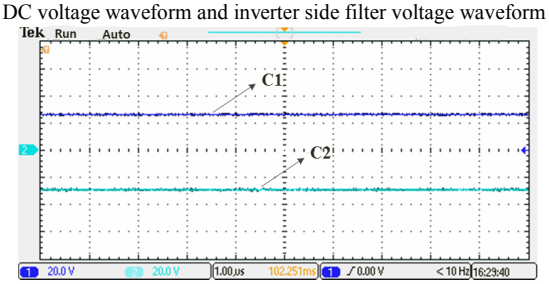

Fig.16. The neutral point voltage experimental waveforms

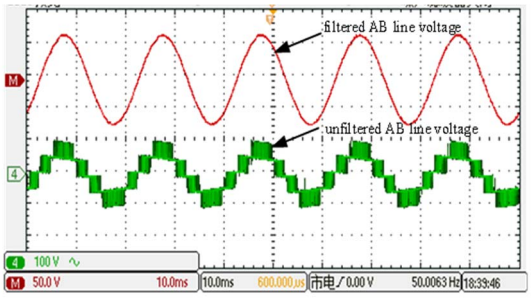

Fig.17 The output AB line voltage experimental waveform

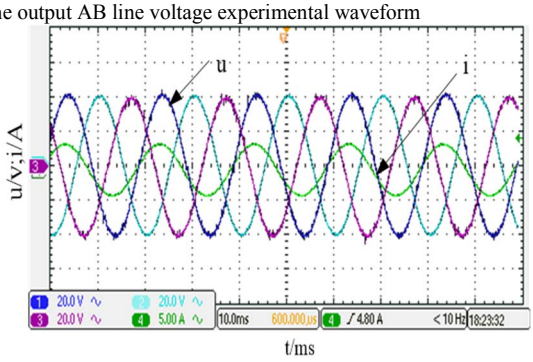

Fig.18 Three-phase filtered output voltage and single-phase output current waveforms

VI. CONCLUSION

In this paper, a model predictive direct power control scheme in the DQ rotating coordinate system is proposed based on the improved T-type three- level inverter topology. The decoupling of active power and reactive power is realized in the DQ rotating coordinate system, and the calculation of active power and reactive power is simplified to improve the system response speed. At the same time, 27 space voltage vectors are divided into the two groups not only save the prediction of the neutral point voltage but also reduce the number of rolling optimization in the control process, which greatly simplifies the calculation and makes the control of the neutral point voltage more direct and effective. Combining theory with practice, an experimental platform was set up to complete the grid-connected operation based on the model predictive direct power control in unit power factor .

REFERENCES

[1] Wang Y.Shi W W，Xie N.et al,"Diode-Free T-Type Three-Level Neutral-Point-Clamped Inverter for Low-Voltage Renewable Energy System," IEEE Transactions on Industrial Electronics，vol. 61, no.11, pp. 6168-6174,Nov. 2014

[2] Bartolomeo Stellato，Tobias Geyer，and Paul J．Goulart,"High-Speed Finite Control Set Model Predictive Control for Power Electronics,"IEEE Transactions on Power Electronics，vol. 32, no.5, pp.4007-4020, May. 2017.

[3] Wang Wan-Cheng，Liu Tian-Hua，Yuddy Syaifud,"Model Predictive Controller for a Micro-PMSM-Based Five-Finger Control System," IEEE Transactions on Industrial Electronics，vol.63, no.6, pp.3666-3676, June. 2016.

[4] Yaramasu V，Wu B,"Predictive Control of a Three-Level Boost Converter and an NPC Inverter for High-Power PMSG-Based Medium Voltage Wind Energy Conversion Systems,"IEEE Transactions on Power Electronics，vol. 29, no.10, pp.5308-5322, Oct. 2014.

[5] Omar Abdel-Rahim, Masato Takeuchi, Hirohito Funato, and Haruna Junnosuke.T-Type Three-Level Neutral Point Clamped Inverter with Model Predictive Control for Grid- Connected Photovoltaic Applications. Presented at International Conference on Electrical Machines and Systems (ICEMS).

[6] CHEN Jing, XIANG Zi-Xin, DENG Yi,"Predictive Direct Power Control of Photovoltaic In-grid Inverted Finite State Model,"Electric Transmission,vol. 47, no.11, pp. 41-44, Nov. 2017.

[7] Jin Nan, Deng Xuanxuan, Cui Guangzhao, et al,"Study on direct power control method for PV grid-connected inverter model prediction," .Journal of Electrical Engineering, vol. 11,no.6, pp.13-18, June. 2016.

[8] HE Peng-fei, GUAN Ping, DONG Ling-ling, YANG Xiu-yuan,"Direct power control of terminal sliding mode variable structure of doubly-fed wind turbine ,"china.electrotechnique, vol. 2017,no.9, pp.92-95, Sept. 2017.

[9] Guan Ping, Dong Lingling, Yang Xiuyuan,"Direct power control for terminal sliding mode variable structure of doubly-fed wind turbine," Power Electronics .vol.2017,no.9,pp.92-95, Sept. 2017

[10] James Scoltock, Tobias Geyer, Senior ,Udaya K,"Madawala Model Predictive Direct Power Control for Grid-Connected NPC Converters," IEEE Transactions on Industrial Electronics, vol. 62, no.9,pp.5319-5328, Sept. 2015.

[11] Dae-Keun Choi, Kyo-Beum Lee,"Dynamic Performance Improvement of AC/DC Converter Using Model Predictive Direct Power Control With Finite Control Set,"IEEE Transactions on Industrial Electronics, vol. 62,no.2, pp.757-767, Feb. 2015.

[12] Xiaohe Wang ,Dan Sun,"Three-Vector-Based Low-Complexity Model Predictive Direct Power Control Strategy for Doubly Fed Induction Generators,"IEEE Transactions on Industrial Electronics, vol. 32, no.1,pp.773-782, Jan. 2017.

[13] Liang Yingyu, Yang Qixun, Liu Jianzheng, et al,"Unbeat-beat direct power control of MMC-HVDC when grid voltage is not balanced,"Transactions of the Chinese Society of Electrotechnical Society, vol. 30,no.15, pp.15-25, Aug. 2015.

[14] Zhou Xiangyu, Zhang Guorong,"A Neutral point Voltage Balance Control Strategy Based on SVPWM for Three-level Inverter ,"Electric and Energy Efficiency Management Technology, vol. 2016,no.9, pp.41-47, May. 2016.

[15] WANG Mei-ling, WANG Li-mei, SUN Yong-liang,"A Neutral point Potential Balance Control Method Based on Model Predictive Control for T-type Three-level Inverter,"Journal of Electrical Engineering, vol. 15, pp.66-72, Sept. 2015.

[16] Li Minyu, Wang Jialiang, Wei Shuguang, et al,"Study on neutral point voltage balance strategy for T-type three-level inverter ,"china.electronictechnology, vol. 2017,no.4, pp.28-30, Apr. 2017.

[17] Jiang Weidong, Wang Qunjing, Chen Quan, et al,"A space vector modulation method for mid-level box-type three-level inverter with neutral point voltage unbalance,"Proceeding of the CSEE, vol.28,no.30,pp.20-26, Oct. 2008.

[18] Lu Jianguo, Wu Fuyun, Hu Wenbin, et al,"Middle-point voltage balance control method for SPWM three-level inverter with dynamic search and modulation modulation bias,"Electric Power Automation Equipment, vol.35,no.12, pp.73-79, Dec. 2015.

[19] Wu Lei,"Three-level Inverter Based on Predictive Direct Power Control,"Journal of Jiangnan University, vol. 14,no.5, pp.562-566, Oct. 2015.

[20] Wu Guoxiang, Yang Yong,"No beat power control in dq rotating coordinate system of three-phase photovoltaic grid-connected inverter,"Journal of Electric Machines and Control,vol. 18,no.12, pp.37-43, Dec. 2014.

[21] Keyuan Huang Shoudao Huang Feng She Baimin Luo Luoqiang Cai. A Control Strategy for Direct-drive Permanent-magnet Wind-power Generator Using Back-to-back PWM Converter.Presented at International Conference on Electrical Machines and Systems.

[22] Yongchang Zhang, Donglin Xu, Jiali Liu, Suyu Gao,"Performance Improvement of odel-Predictive Current Control of Permanent Magnet Synchronous Motor Drives,"IEEE Transactions on Industrial Electronics,vol. 32,no.2, pp.3683-3695, Jan. 2017.

[23] Tianshi Wang , Chengcheng Liu , Gang Lei,"Model predictive direct torque control of permanent magnet synchronous motors with extended set of voltage space vectors,"IET Electric Power Applications,vol.11,no.8, pp.1376-1382, June. 2017.

[24] Yin Shi. Tan Guosun,"MMC Simplified Finite Set Fast Model Predictive Control,"Power Electronics,vol.49,no.11, pp.60-62, Nov. 2015.

[25] Soeiro T B, Kolar J W,"The New High-Efficiency Hybrid Neutral-Point-Clamped Converter," IEEE Transactions on Industrial Electronics, vol. 60, no.5, pp.1919-1935, May. 2013.

Guoliang Yang(M'17) received the B.S., M.S., and Ph.D. degrees in electrical engineering from Yanshan University, Qinhuangdao, China, in 1996, 2002, and 2009 respectively. In 2002, he joined the Department of Electrical Engineering and Automation, Yanshan University, where he has been an Associate Professor of electrical engineering since 2011. He was a visiting scholar at the Department of Energy Technology in Aalborg University, Denmark from september, 2017 to september,2018.

His current major research interests include motor drive,power electronics design, wind power generation system, micro-grid and its control.

Shuai Hao received the B.E. degree in electrical engineering from Liren College,Yanshan University, Hebei, China,in 2016. She is currently pursuing the Master degree in electrical engineering at the departmet of Electrical Engineering of Yanshan University.

Her research interest includes the new energy generation technology, inverter grid control, and multilevel converter.

Chuntian Fu received the B.E. degree in electrical engineering from Liren College, Yanshan University, Hebei, China, in 2015. He is currently pursuing the Master degree in electrical engineering at the departmet of Electrical Engineering of Yanshan University.

His research interest includes the new energy generation technology, inverter grid control, and multilevel converter .

Zhe Chen (M'95–SM'98) received the B.Eng. And M.Sc. degrees in electrical engineering from the Northeast China Institute of Electric Power Engineering, Jilin City, China, the M.Phil. degree in power electronics from Staffordshire University, England, U.K., and the Ph.D. degree in power and control from the University of Durham, England.

He is currently a Full Professor with the Department of Energy Technology, Aalborg University, Aalborg,

Denmark, where he is the Leader of the Wind Power System Research program. He is the Danish Principle Investigator for Wind Energy of Sino-Danish Centre for Education and Research. His current research interests include power systems, power electronics, and electric machines and wind energy and modern power systems. He has led many research projects and has more than 400 technical publications with more than 10 000 citations and h-index of 44 (Google Scholar).

Dr. Chen is an Associate Editor of the IEEE Transactions on Power Electronics. He is a Fellow of the Institution of Engineering and Technology (London, U.K.) and a Chartered Engineer in the U.K.